

***In situ* fluorescence experiments to study swelling and slow release kinetics of disc-shaped poly(methyl methacrylate) gels made at various crosslinker densities**

Y. Yilmaz and Ö. Pekcan*

*Department of Physics, Istanbul Technical University, Maslak 80626, Istanbul, Turkey
 (Received 6 March 1997; revised 7 July 1997, accepted 4 September 1997)*

In situ steady state fluorescence (SSF) measurements are performed for studying swelling and slow release processes in gels formed by free radical crosslinking copolymerization (FCC) of methyl methacrylate (MMA) and ethylene glycol dimethacrylate (EGDM). Gels were prepared at 80°C for various EGDM contents with pyrene (Py) as a fluorescence probe. After drying these gels, swelling and slow release experiments were performed in chloroform at room temperature by real-time monitoring of the Py fluorescence intensity. A correction method was developed to obtain pure swelling curves, by using desorption curves of Py molecules. The Li–Tanaka equation was employed to produce swelling parameters. Cooperative diffusion coefficients (D_c) were measured and found to be around 2×10^{-5} cm²/s for gels swollen in chloroform. Slow release diffusion coefficients (D) were measured using the classical diffusion equation and found to be around 8×10^{-5} cm²/s. © 1998 Elsevier Science Ltd. All rights reserved.

(Keywords: poly(methyl methacrylate) gels; steady state fluorescence; kinetics)

INTRODUCTION

Polymer networks or gels are known to exist generally in two forms, swollen and shrunken. Volume transitions occur between these forms either continuously or in sudden jumps^{1,2}. The equilibrium swelling and shrinking of gels in solvents has been extensively studied^{3–5}. The swelling, shrinking and drying kinetics of physical and chemical gels are very important in many technological applications: in the pharmaceutical industry in designing slow-release devices for oral drugs; understanding the mechanism of swelling, shrinking and drying kinetics is highly desirable in the use of cosmetics ingredients; in the agricultural industry for producing storable foods; and in medical applications in developing artificial organs.

The swelling properties of chemically crosslinked gels can be understood by considering the osmotic pressure *versus* the restraining force^{6–10}. The total free energy of a chemical gel consists of bulk and shear energies. In fact, in a swollen gel the bulk energy can be characterized by the osmotic bulk modulus K , which is defined in terms of the swelling pressure and the volume fraction of polymer at a given temperature. The shear energy which keeps the gel in shape can be characterized by shear modulus G . Here shear energy minimizes the non-isotropic deformations in gel. The theory of kinetics of swelling for a spherical chemical gel was first developed by Tanaka *et al.*¹¹ where the assumption is made that the shear modulus, G is negligible compared to the osmotic bulk modulus. Later, Peters *et al.*¹² derived a model for the kinetics of swelling in spherical and cylindrical gels by assuming non-negligible shear modulus. Recently Li and Tanaka⁶ have developed a model where the shear modulus plays an important role which keeps the gel in shape due to coupling of any change in different directions. This model

predicts that the geometry of the gel is an important factor, and swelling is not a pure diffusion process.

Several experimental techniques have been employed to study the kinetics of swelling, shrinking and drying of chemical and physical gels, among which are neutron scattering¹³, quasilastic light scattering¹², macroscopic experiments⁷ and *in situ* interferometric¹⁴ measurements. Recently, by measuring the Stokes shift of a polarity sensitive fluorescence species, the gelation during epoxy curing was monitored as a function of cure time¹⁵. Time-resolved and steady state fluorescence techniques were employed to study isotactic polystyrene in its gel state¹⁶ where excimer spectra were used to monitor the existence of two different conformations in the gel state of polystyrene. A pyrene derivative was used as a fluorescence molecule to monitor the polymerization, aging and drying of aluminosilicate gels¹⁷. These results were interpreted in terms of the chemical changes occurring during the sol–gel process and the interactions between the chromophores and the sol–gel matrix. Recently we reported *in situ* observations of the sol–gel phase transition in free radical crosslinking copolymerization, using the fluorescence technique^{18–20}. The same technique was also performed for studying swelling and drying kinetics in disc-shaped gels^{21,22}. In this paper swelling and slow release kinetics of gels formed by free radical crosslinking copolymerization (FCC) of methyl methacrylate (MMA) and ethylene glycol dimethacrylate (EGDM) are studied. Pyrene (Py) is used as a fluorescence probe to monitor swelling and slow release processes during *in situ* fluorescence experiments in chloroform.

THEORETICAL CONSIDERATIONS

It has been suggested⁶ that the kinetics of swelling and shrinking of a polymer network or gel should obey the

* To whom correspondence should be addressed

following relationship:

$$\frac{W(t)}{W_\infty} = 1 - \sum_{n=1}^{\infty} B_n e^{-t/\tau_n} \quad (1)$$

where $W(t)$ and W_∞ are the swelling or solvent uptake at time t and at infinite equilibrium, respectively. $W(t)$ can also be expressed as a volume difference of the gel at time t and zero. Each component of the displacement vector of a point in the network from its final equilibrium location after the gel is fully swollen, decays exponentially with a time constant τ_n which independent of time t .

Here B_n is given by the following relationship⁶:

$$B_n = \frac{2(3-4R)}{\alpha_n^2 - (4R-1)(3-4R)} \quad (2)$$

where R is defined as the ratio of the shear and the longitudinal osmotic modulus, $R = G/M$. The longitudinal osmotic modulus, M is a combination of shear modulus G , and osmotic bulk modulus K , $M = K + 4G/3$, and α_n is given as a function of R as follows:

$$R = \frac{1}{4} \left[1 + \frac{\alpha_n J_0(\alpha_n)}{J_1(\alpha_n)} \right] \quad (3)$$

where J_0 and J_1 are the Bessel functions.

In equation (1), τ_n is inversely proportional to the collective cooperative diffusion coefficient D_c of a gel disc at the surface and is given by⁷:

$$\tau_n = \frac{3a^2}{D_c \alpha_n^2} \quad (4)$$

where the diffusion coefficient D_c is given by $D_c = M/f = (K + 4G/3)/f$, f being the friction coefficient describing the viscous interaction between the polymer and the solvent, and a represents half of the disc thickness in the final infinite equilibrium which can be experimentally determined.

The series given by equation (1) is convergent. The first term of the series expansion is dominant at large t , which corresponds to the last stage of the swelling. As it is seen from equation (4) τ_n is inversely proportional to the square of α_n , where α_n are the roots of the Bessel functions. If $n > 1$, α_n increases and τ_n decreases very rapidly. Therefore in the limit of large t or if τ_1 is much larger than the rest of τ_n , all high-order terms ($n \geq 2$) in equation (1) can be dropped so that the swelling and shrinking can be represented by first-order kinetics¹⁴. In this case equation (1) can be written as

$$\frac{W(t)}{W_\infty} = 1 - B_1 e^{-t/\tau_1} \quad (5)$$

This equation allows us to determine the parameters B_1 and τ_1 .

Here it is important to note that equation (5) satisfies the following:

$$\frac{dW(t)}{dt} = \frac{1}{\tau_1} (W_\infty - W) \quad (6)$$

which suggests that the process of swelling should obey first-order kinetics. The higher-order terms ($n \geq 2$) can be considered as fast decaying perturbative additions to the first-order kinetics of the swelling in the limit of large t .

EXPERIMENTS

EGDM has been commonly used as crosslinker in the synthesis of polymeric networks²³. Here, for our use, the monomers MMA (Merck) and EGDM (Merck) were freed from the inhibitor by shaking with a 10% aqueous KOH solution, washing with water and drying over sodium sulfate. They were then distilled under reduced pressure over copper chloride. Then radical copolymerization of MMA and EGDM was performed in bulk at 80°C in the presence of 2,2'-azobisisobutyronitrile (AIBN) as an initiator. AIBN (0.26 wt%) was dissolved in MMA and this stock solution was divided and transferred into round glass tubes of 9.5 mm internal diameter. Py was added as a fluorescence probe before the gelation process. Here Py concentration was taken as 4×10^{-4} M. Five different samples were prepared using this stock solution with various EGDM contents. Details of the samples are listed in Table 1. All samples were deoxygenated by bubbling nitrogen for 10 min and then radical copolymerization of MMA and EGDM was performed. After polymerization we obtained the gels in which probe Py molecules remained.

Steady state fluorescence measurements were carried out using a Perkin Elmer Model LS-50 spectrofluorimeter equipped with temperature controller. All measurements were made at the 90° position and slit widths were kept at 2.5 mm. After the gels were formed we cut the gel samples into disc shapes to use in swelling and slow release experiments. *In situ* swelling and slow release experiments were both performed in a 1 cm × 1 cm quartz cell at room temperature. Gel samples were attached to one side of a quartz cell by pressing the disc with thin steal wire. The quartz cell was filled with chloroform. This cell was placed in the spectrofluorimeter and fluorescence emission was monitored at a 90° angle. Two different experiments were carried out for two different positions of the gel samples (see Figure 1). In both experiments identical disc-shaped gels were used which were dried and cut from the cylindrical gels obtained from FCC. The radii of these disc-shaped gels were around 7.7 mm. In the first position only the gel was illuminated by the excitation light where the total fluorescence emission, I_p , caused by Py molecules comes

Table 1 Experimentally produced swelling parameters for the gels prepared at various crosslinker (EGDM) densities

	Gel				
	1	2	3	4	5
Vol% EGDM ($\times 10^{-3}$)	2.5	5	17.5	20	25
τ_1 (s)	2262	1871	1346	1309	1227
B_1	0.51	0.69	0.48	0.69	0.66
R	0.0	0.314	0.0	0.314	0.258
α_1	2.3	1.92	2.30	1.92	2.00
D_c ($\times 10^{-5}$ cm ² /s)	1.8	2.2	1.0	1.7	2.1
a_i (cm)	0.219	0.215	0.197	0.229	0.204
a (cm)	0.538	0.453	0.320	0.338	0.300
$(a - a_i)$ (cm)	0.319	0.238	0.123	0.109	0.096

from the Py immersed in the gel and desorbed from the swelling gel. In the second position the gel sample was shifted slightly upward so that only the cell with chloroform was illuminated by the excitation light. Here the fluorescence emission, I_d , from Py molecules which are desorbed from the swelling gel was monitored. *Figure 1a* and *b* show the first and second position of the gels, respectively.

During the experiments the wavelength of the excitation light was kept at 345 nm and Py fluorescence intensities were monitored at 395 nm using the 'time drive' mode of the spectrofluorimeter. No shift was observed in the wavelength of maximum intensity of Py emission and gel samples kept their transparencies during the experiments. Typical fluorescence spectra for the two positions are shown in *Figure 2*. We used desorption curves of Py molecules to obtain pure swelling curves by subtracting the intensities taken from samples at the position given in *Figure 1a* and *b*.

In swelling experiments, continuous volume transitions are expected which should result in continuous decrease in I_p during swelling. Here one may expect that as solvent uptake (W) increases, desorption of Py molecules from the swollen gel increases, as a result Py intensity from the first position decreases. On the other hand during slow release experiments one should expect an increase in I_d , due to an increasing amount of Py molecules which are released into the chloroform in the cell.

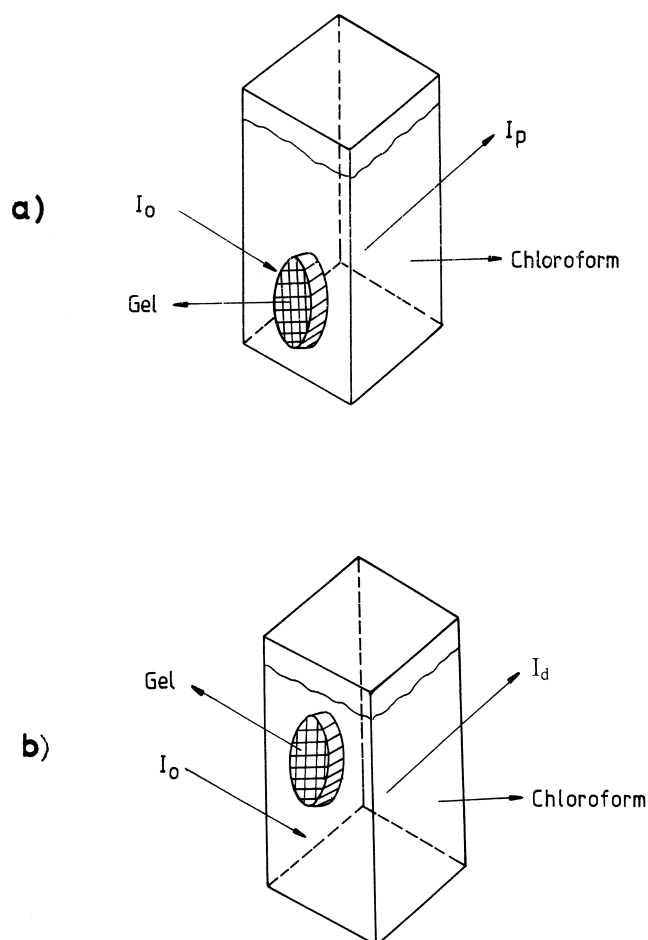


Figure 1 Fluorescence cell in LS-50 Perkin Elmer spectrofluorimeter. Monitoring of (a) the first position and (b) the second position (desorption processes) of the gel explained in the text. I_0 and I_p are the excitation and emission intensities at 345 and 395 nm, respectively

RESULTS AND DISCUSSION

Swelling

A close analogy exists between swelling equilibrium and osmotic equilibrium. The elastic reaction of the network structure may be interpreted as a pressure acting on the swollen gel. In the equilibrium state this pressure is sufficient to increase the chemical potential of the solvent in the gel so that it is equal to that of the excess solvent surrounding the swollen gel. Thus the network structure plays the multiple role of solute, osmotic membrane, and pressure-generating device²⁷. Therefore, the motion of the probe molecules in terms of their physical force can be understood by means of osmotic pressure or chemical potential. Before the swelling equilibrium the difference of the chemical potentials between the inside and outside of the gel should ensure that the Py molecules are washed out of the gel. Here it may be assumed that Py molecules are not completely washed out from the swollen part of the gel. But in our case, since the volume of the quartz cell (4 ml) which was filled completely with chloroform is approximately 40 times larger than the volume of the disc-shaped gels at

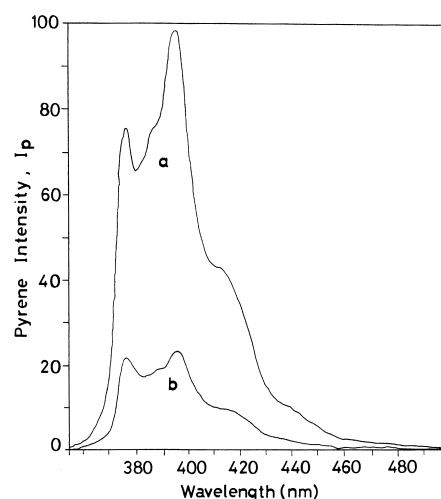


Figure 2 Emission spectra of Py taken from the gel at position 1: (a) before and (b) after the swelling process is completed. Py is excited at 345 nm

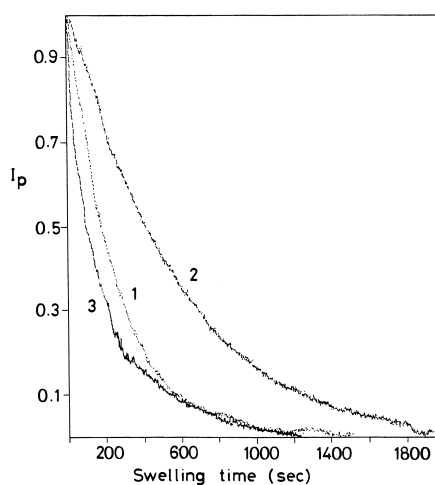


Figure 3 Total Py intensity, I_p , versus swelling time for the gel samples listed in *Table 1*. The gel in the cell was illuminated at 345 nm (at position 1) during swelling measurements. Data for the plot were obtained using the time drive mode of the spectrofluorimeter

equilibrium state, than the intensity that comes from this swollen part of the gel can be ignored.

Pyrene intensities in the first position of the gel *versus* time are plotted in *Figure 3*. The numbers in *Figure 3* correspond to gel samples listed in *Table 1*. The curves in *Figure 3* were obtained during *in situ* fluorescence experiments shown in *Figure 1a*, where at the beginning all Py molecules are in the gel and I_{os} is obtained. After solvent penetration starts, some Py molecules are washed out from the swollen part of the gel into the cell; as a result Py intensity, I_s , from the glassy gel decreases as swelling time increases. At the equilibrium state of swelling, Py intensity from the glassy gel reaches a value $I_{\infty s}$ where the solvent uptake by swollen gel is W_{∞} . The schematic representation of these swelling stages is shown in *Figure 4* where the intensities from the desorbed Py molecules are given by I_d . The relation between solvent uptake W and fluorescence intensity I_s from the glass part of the gel is given by the following:

$$\frac{W}{W_{\infty}} = \frac{I_{os} - I_s}{I_{os} - I_{\infty s}} \quad (7)$$

Since $I_{os} \gg I_{\infty s}$, then equation (7) becomes

$$\frac{W}{W_{\infty}} = 1 - \frac{I_s}{I_{os}} \quad (8)$$

This equation predicts that as W increases I_s decreases and is quite similar to the equation used to monitor oxygen uptake by poly(methyl methacrylate) and poly(vinyl acetate) spheres^{24,25}.

Combining equations (8) and (5) the following useful relationship can be obtained:

$$\ln\left(\frac{I_s}{I_{os}}\right) = \ln B_1 - \frac{t}{\tau_1} \quad (9)$$

If one thinks that the fluorescence intensity curves in *Figure 3* are originated only from the gels, then equation (9) has to be obeyed by the data. When the digitized form of the data in *Figure 3* are plotted using equation (9), one fails to observe the linear relationship in the swelling curves. This is not surprising²¹ because, during the swelling experiments, desorbing Py molecules also contribute to the fluorescence intensity, which prevents us from observing pure swelling curves as shown in *Figure 4*. In fact the data in *Figure 3* present the total Py intensity, I_p curves, during *in situ* swelling experiments, which are given by the following:

$$t = 0, I_{op} = I_{os} + I_{od} \quad (10)$$

$$t > 0, I_p = I_s + I_d$$

$$t = \infty, I_{op} = I_{\infty s} + I_{\infty d}$$

where I_d is the Py intensity from the desorbing Py molecules as shown in *Figure 4*. Plots of I_d *versus* desorbing time for three different gels are shown in *Figure 5* which are obtained from the experiments performed according to *Figure 1b*. In *Figure 5*, I_d increases as slow release time increases for all the gel samples. Here the numbers represents the gels given in *Table 1* and in *Figure 3*. Since I_d is directly proportional to the number of Py molecules in chloroform, the behaviour of the intensity curves in *Figure 5* suggest that Py molecules are slow released much faster from densely formed gel (3) than loosely formed gels (1 and 2). (Here gels with high EGDM content are named as densely formed gels.)

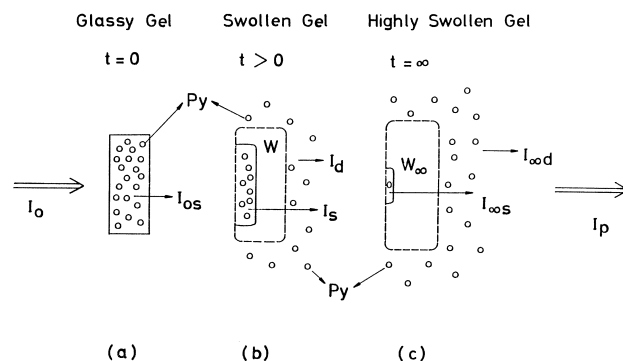


Figure 4 Schematic representation of the swelling processes in the gel during solvent uptake. Fluorescence intensities from Py molecules are also presented. (a) Gel before swelling; I_{os} is the fluorescence intensity from glassy gel at $t = 0$. (b) Swollen gel; I_s and I_d are the fluorescence intensities from glassy gel and desorbed Py molecules at $t > 0$, W is the solvent uptake. (c) Highly swollen gel; $I_{\infty s}$ and $I_{\infty d}$ are the fluorescence intensities at $t = \infty$, W_{∞} is the solvent uptake at $t = \infty$

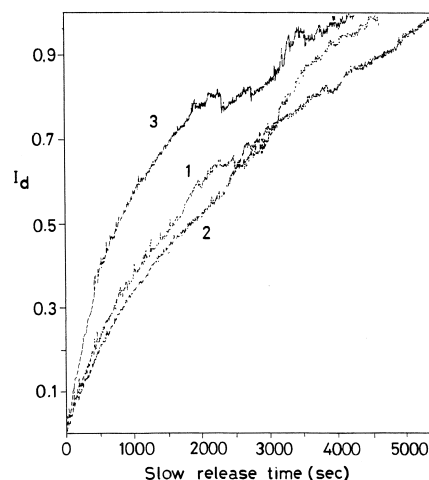


Figure 5 Py intensity, I_d , from desorbing Py molecules *versus* slow release time for the gel samples listed in *Table 1*. The cell was illuminated (position 2) at 345 nm during desorption measurements. Data were obtained using the time drive mode of the spectrofluorimeter

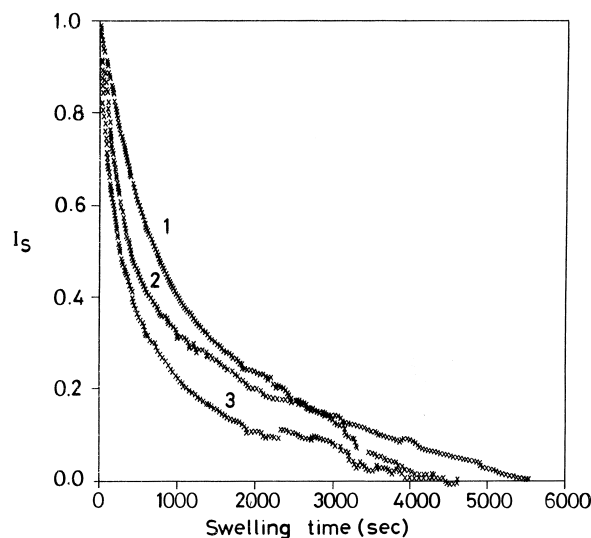


Figure 6 Py intensity, I_s , from glassy part of the gel which is obtained by subtracting the data in *Figure 3* from the data in *Figure 5*

In order to produce the pure swelling intensity (I_s) curves, data in Figure 5 are subtracted from the data in Figure 3 according to equation (10) and plotted in Figure 6. For confirming the correctness of the pure swelling curves, data in Figure 6 are digitized according to equation (9) and plotted in Figure 7, where linear relationships are obtained except at very short and long time regions. Long time deviations are explained by the saturation of solvent uptake. Short time deviations may correspond to fast relaxation processes in the gel at an early swelling stage. Equation (5) is not used for short regions. Using equation (9) linear regression of curves in Figure 7 at intermediate times provides us with B_1 and τ_1 values. Fits are shown in Figure 8. Taking into account the dependence of B_1 on R , one obtains R values and from α_1 - R dependence α_1 values were produced⁶. Then using equation (4) for $n = 1$, cooperative diffusion coefficients D_c were determined for these disc-shaped gels and found to be around 2×10^{-5} cm²/s. Experimentally obtained parameters τ_1 and B_1 , together with α_1 and D_c values are summarized in Table 1, where a values are also presented for each gel. Here one should notice that measured D_c values are found to be similar for loosely and densely formed gels. However, τ_1 values in Table 1 show smaller τ_1 values for densely formed gels than for loosely formed gels.

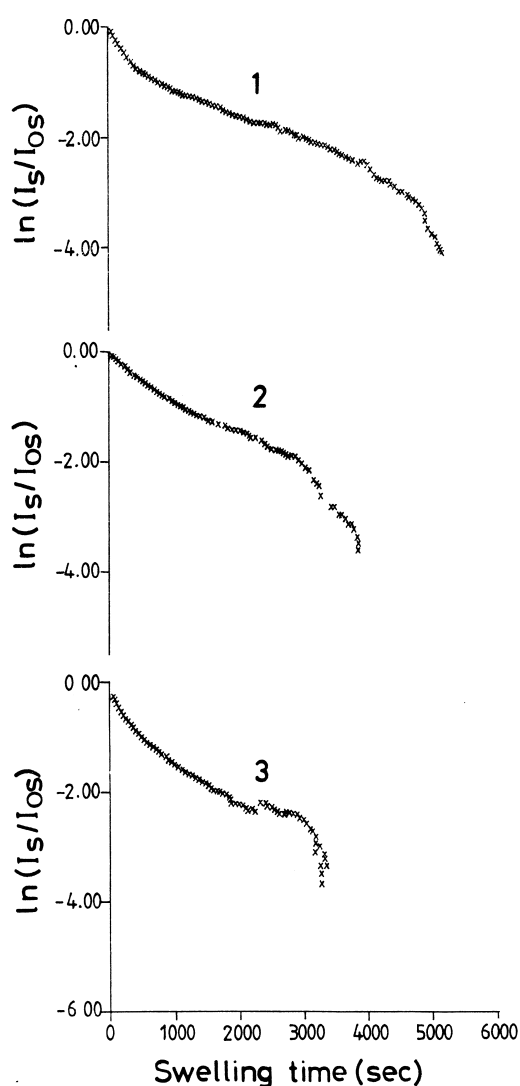


Figure 7 Logarithmic plot of the digitized data of Figure 6, which obey equation (9). (a-c) Data for the gel samples marked with 1, 2 and 3 in Figure 6 and Table 1

As the network is swollen by absorption of solvent, the chains between network junctions are required to assume elongated configurations, and a force akin to the swelling process. As swelling proceeds this force increases and the dilution force decreases. The force of the retraction in a stretched network structure depends also on the degree of crosslinking²⁷. The degree of swelling observed at equilibrium in a good solvent invariably decreases with increasing degree of crosslinking. The fact that densely formed gels show smaller τ_1 values than loosely formed gels can be understood by realizing the fact that loosely formed gels are more flexible, which can take more solvent easily and need longer times to reach a fully swollen state. In other words the release of Py from dense and loose gels may be understood in terms of different osmotic stress induced by tighter and looser gels, respectively. As the crosslinker density of the gels decreases, elastic contribution to the osmotic pressure which drives the solvent out also decreases and the swelling (solvent uptake) increases. The variation in the final (a) and initial (a_i) disc thicknesses ($a - a_i$) are also summarized in Table 1, where one can see that loosely formed gels swelled much more than densely formed gels.

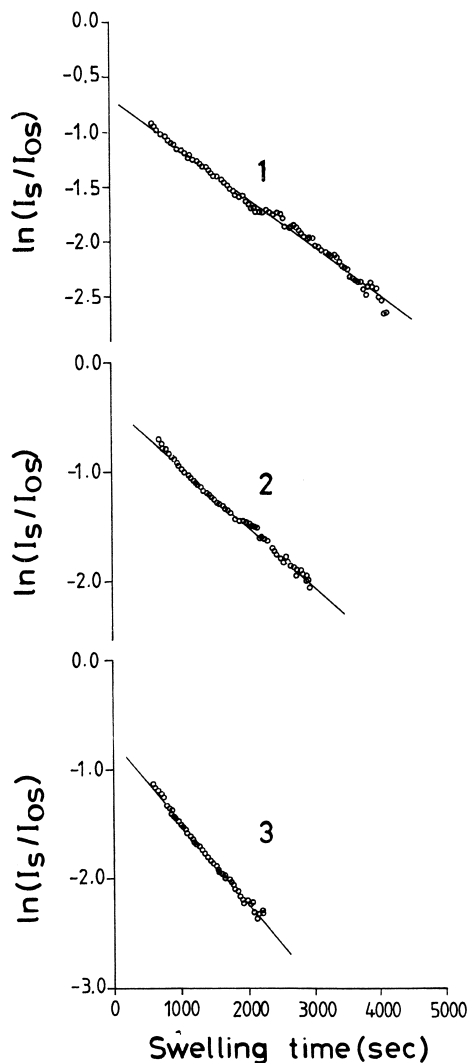


Figure 8 Linear regressions of the data presented in Figure 7 at the intermediate time regions. B_1 and τ_1 values were obtained from the intersections and the slopes of the plots in (a-c) for the gels marked with 1, 2 and 3 in Figure 7

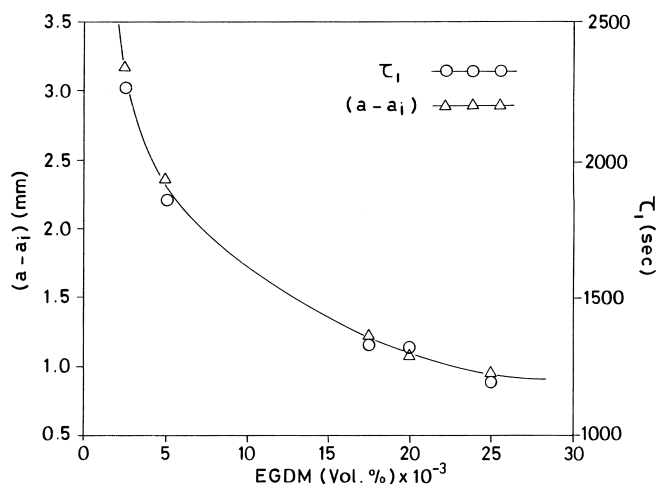


Figure 9 Plot of τ_1 and $(a - a_i)$ values versus EGDM content for the gel samples listed in Table 1

Table 2 Experimentally produced slow release diffusion coefficients (D) for the gels prepared at various crosslinker (EGDM) densities

	Gel				
	1	2	3	4	5
Vol% EGDM ($\times 10^{-3}$)	2.5	5	17.5	20	25
D ($\times 10^{-5}$ cm ² /s)	6.31	5.48	8.21	7.52	13.2
a_i (cm)	0.219	0.215	0.197	0.229	0.204
a (cm)	0.538	0.453	0.320	0.338	0.300

For illustration, τ_1 and $(a - a_i)$ values versus EGDM content are plotted in Figure 9, where the agreement between τ_1 and $(a - a_i)$ values versus EGDM content can be observed. Here we note that no correlation between D_c values and EGDM content was observed for the gels used in this work.

Slow release

Figure 5 presents the results of the slow release experiments where Py intensity, I_d , increases as slow release (desorption) time increases for all the gel samples. Here numbers represent the gels given in Tables 1 and 2. Since I_d is directly proportional to the number of Py molecules in chloroform, the behaviour of the intensity curves in Figure 5 suggest that Py molecules are released much faster from densely formed gels (3) than loosely formed gels (1 and 2). This behaviour is similar to the swelling curves in Figure 6, where densely formed gels (3) showed faster uptake than loosely formed gels. At this point, one can reach a conclusion that slow release of Py molecules takes place during the swelling processes of the gel. Under this picture the slow release process can be treated using the Fickian diffusion model. Curves in Figure 5 also support this suggestion where they show purely Fickian behaviour. The desorption transport from a thin slab of thickness l is given by the following²⁶:

$$\frac{M_t}{M_\infty} = 1 - \frac{8}{\pi^2} \sum_{n=0}^{\infty} \frac{1}{(n+1)^2} \exp\left(-\frac{(2n+1)^2 D \pi^2 t}{l^2}\right) \quad (11)$$

where D is the desorption diffusion coefficient, M_t represents the amount of material released at time t and M_∞ is its equilibrium value at $t = \infty$. In order to interpret our findings l

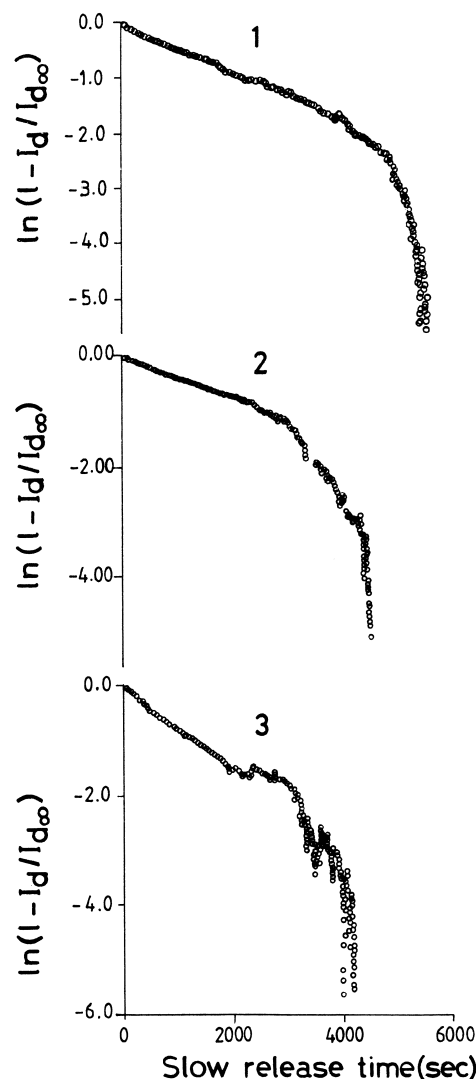


Figure 10 Logarithmic plot of the digitized data in Figure 5 which obey equation (12). (a–c) Data for the gel samples marked with 1, 2 and 3 in Figure 5 and in Table 2

is taken as the initial thickness (a_i) of the swollen gel. M_t and M_∞ can be considered to be proportional to I_d and $I_{d\infty}$, respectively during the slow release process, where the disk-shaped gels are assumed to be thin slabs. The logarithmic

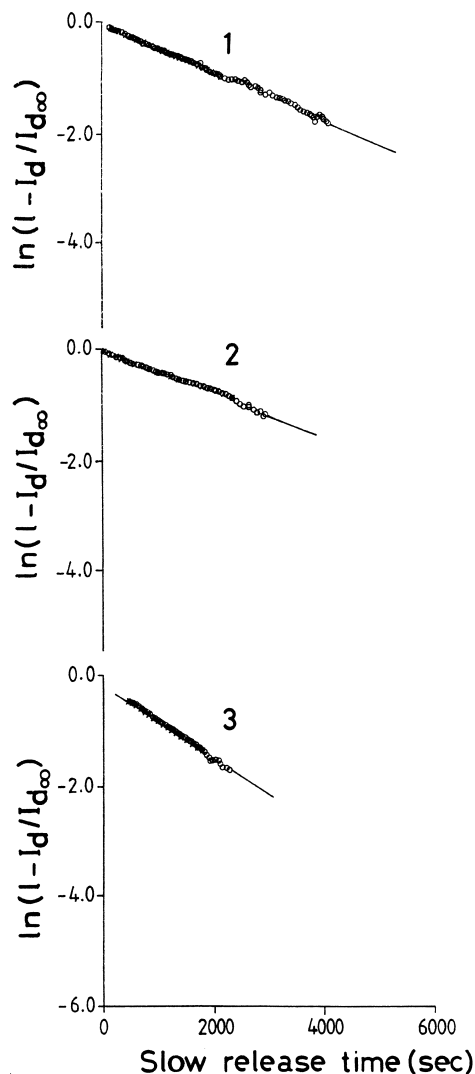


Figure 11 Linear regression of the data presented in Figure 10. D values were obtained from the slopes of the plots in (a–c) marked with 1, 2 and 3 in Figure 10

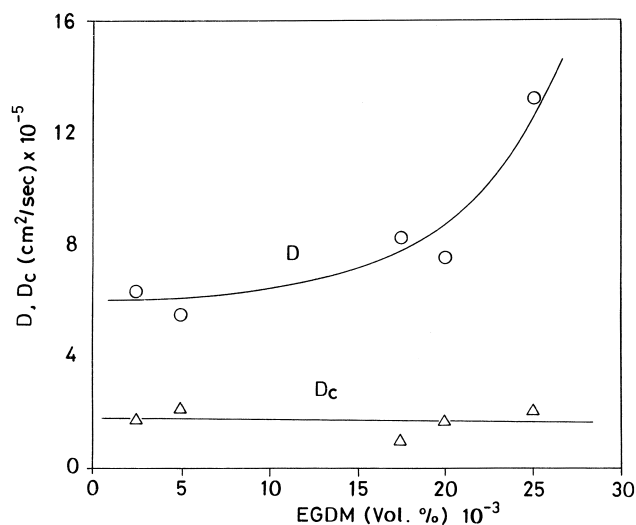


Figure 12 Plot of D_c and D values versus EGDM content for the gel samples listed in Tables 1 and 2

form of equation (11) for $n = 0$ can be given as follows:

$$\ln\left(1 - \frac{I_d}{I_{d\infty}}\right) = \ln\left(\frac{8}{\pi^2}\right) - \frac{D\pi^2}{a^2}t \quad (12)$$

Slow release diffusion coefficients now can be obtained for Py molecules by digitizing the data in Figure 5 using equation (12). Results are plotted in Figure 10, where linear relationships can be seen, except at long time regions which correspond to saturation of slow release processes. Using equation (12) linear regression of curves in Figure 10 produces D values which are listed in Table 2 and fits are shown in Figure 11. As expected, D values for the loosely formed gels (1 and 2) are found to be smaller than the densely formed gels (5 and 6), i.e. slow release of Py molecules is much slower from the flexible gel than from a rigid gel, which can be explained by the higher shear energies in rigid gels. However, at this stage of our work we are unable to interpret the behaviour of cooperative diffusion coefficients D_c of disc-shaped gels. One may argue that the phantom characteristic of a gel may cause this behaviour of D_c values versus crosslinker density. In Figure 12 the behaviour of D and D_c values are summarized versus EGDM content.

In conclusion these results have shown that the direct fluorescence method can be used for real-time monitoring of the swelling and slow release processes. In this method *in situ* fluorescence experiments are easy to perform and provide us with quite sensitive results to measure the swelling and slow release parameters.

ACKNOWLEDGEMENTS

We thank Professor O. Okay for providing us with the material and stimulating ideas.

REFERENCES

1. Duşek, K. and Paterson, D., *J. Polym. Sci.*, 1968, **A26**, 1209.
2. Tanaka, T., *Phys. Rev. Lett.*, 1980, **45**, 1636.
3. Tobolsky, A. V. and Goebel, J. C., *Macromolecules*, 1970, **3**, 556.
4. Schild, H. G., *Prog. Polym. Sci.*, 1992, **17**, 163.
5. Amiya, T. and Tanaka, T., *Macromolecules*, 1987, **20**, 1162.
6. Li, Y. and Tanaka, T., *J. Chem. Phys.*, 1990, **92**(2), 1365.
7. Zrinyi, M., Rosta, J. and Horkay, F., *Macromolecules*, 1993, **26**, 3097.
8. Candau, S., Baltide, J. and Delsanti, M., *Adv. Polym. Sci.*, 1982, **7**, 44.
9. Geissler, E. and Hecht, A. M., *Macromolecules*, 1980, **13**, 1276.
10. Zrinyi, M. and Horkay, F., *J. Polym. Sci., Polym. Ed.*, 1982, **20**, 815.
11. Tannaka, T. and Filmore, D., *J. Chem. Phys.*, 1979, **20**, 1214.
12. Peters, A. and Candau, S. J., *Macromolecules*, 1988, **21**, 2278.
13. Bastide, J., Duoplessix, R., Picot, C. and Candau, S., *Macromolecules*, 1984, **17**, 83.
14. Wu, C. and Yan, C.-Y., *Macromolecules*, 1994, **27**, 4516.
15. Lin, K. F. and Wang, F. W., *Polymer*, 1994, **4**, 687.
16. Wandelt, B., Birch, D. J. S., Imhof, R. E., Holmes, A. S. and Pethnick, R. A., *Macromolecules*, 1991, **24**, 5141.
17. Panxviel, J. C., Dunn, B. and Zink, J. J., *J. Phys. Chem.*, 1989, **93**, 2134.
18. Pekcan, Ö., Yılmaz, Y. and Okay, O., *Chem. Phys. Lett.*, 1994, **229**, 537.
19. Pekcan, Ö., Yılmaz, Y. and Okay, O., *Polymer*, 1996, **37**, 2049.
20. Pekcan, Ö., Yılmaz, Y. and Okay, O., *J. Appl. Polym. Sci.*, 1996, **61**, 2279.
21. Pekcan, Ö. and Yılmaz, Y., *J. Appl. Polym. Sci.* (in press).
22. Pekcan, Ö. and Yılmaz, Y., *Progr. Colloid Polym. Sci.*, 1996, **102**, 89.
23. Okay, O. and Gürün, Ç., *J. Appl. Polym. Sci.*, 1992, **46**, 421.
24. Kaptan, Y., Pekcan, Ö., Guven, O. and Arca, E., *J. Appl. Polym. Sci.*, 1989, **37**, 2537.
25. Kaptan, Y., Pekcan, Ö. and Guven, O., *J. Appl. Polym. Sci.*, 1992, **44**, 1595.
26. Crank, J. and Park, G. S. *Diffusion in Polymers*. Academic Press, London, 1968.
27. Flory, P. J., *Principles of Polymer Chemistry*. Cornell University Press, Ithaca, NY, 1953.